Journal Pre-proof

Crosstalk between ROS-dependent apoptotic and autophagic signaling pathways in Zn(II) phthalocyanine photodynamic therapy of melanoma

Federico Valli, María C. García Vior, Leonor P. Roguin, Julieta Marino

PII: S0891-5849(19)32565-1

DOI: https://doi.org/10.1016/j.freeradbiomed.2020.01.018

Reference: FRB 14571

To appear in: *Free Radical Biology and Medicine*

Received Date: 20 December 2019

Revised Date: 16 January 2020

Accepted Date: 16 January 2020

Please cite this article as: F. Valli, Marí.C. García Vior, L.P. Roguin, J. Marino, Crosstalk between ROS-dependent apoptotic and autophagic signaling pathways in Zn(II) phthalocyanine photodynamic therapy of melanoma, *Free Radical Biology and Medicine* (2020), doi: https://doi.org/10.1016/j.freeradbiomed.2020.01.018.

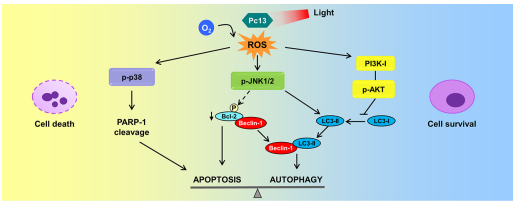

CROSSTALK BETWEEN ROS-DEPENDENT APOPTOTIC AND AUTOPHAGIC SIGNALING PATHWAYS IN ZN(II) PHTHALOCYANINE PHOTODYNAMIC THERAPY OF MELANOMA

Federico Valli [a], María C. García Vior [b], Leonor P. Roguin [a], Julieta Marino [a*]

[a] Universidad de Buenos Aires. Facultad de Farmacia y Bioquímica. Departamento de Química Biológica. CONICET-UBA. Instituto de Química y Fisicoquímica Biológicas (IQUIFIB). Junín 956, C1113AAD, Buenos Aires, Argentina.

[b] Universidad de Buenos Aires. Facultad de Farmacia y Bioquímica. Departamento de Química Orgánica. CONICET. Junín 956, C1113AAD, Buenos Aires, Argentina.

Corresponding author: Julieta Marino

Tel.: +54 11 4964 8290; Fax: +54 11 4962 5457

E-mail address: jmarino@qb.ffyb.uba.ar

ORCID of the authors:

Federico Valli ORCID: 0000-0002-9333-3140

María C. García Vior ORCID: 000-0002-4362-7407

Leonor P. Roguin ORCID: 0000-0002-0293-0477

Julieta Marino ORCID: 0000-0002-1226-448X

Keywords

Zinc phthalocyanine

Cell signaling

Autophagy

Apoptosis

Photodynamic therapy

Melanoma

Abbreviations:

AKT, protein kinase B

CQ, chloroquine

DN, dominant negative

ERK, extracellular signal-regulated kinase

FBS, fetal bovine serum

JNK, c-Jun N-terminal kinase

LC3-II, microtubule-associated protein 1 light chain 3 II

3-MA, 3-methyladenine

MAPK, mitogen-activated protein kinase

PARP-1, poly(ADP-ribose) polymerase

PBS, phosphate buffered saline

Pc, phthalocyanine

PDT, photodynamic therapy

p.i., post irradiation

PI3K, phosphatidylinositol 3-kinase

PS, photosensitizer

ROS, reactive oxygen species

Trolox, 6-hydroxy-2,5,7,8-tetramethylchroman-2-carboxylic acid

WM, wortmannin

Abstract

Melanoma is the most aggressive type of skin cancer, highly resistant to conventional therapies. Photodynamic therapy (PDT) is a minimally invasive treatment modality that combines the use of a photosensitizer, visible light and molecular oxygen, leading to ROS generation in the specific site of irradiation. The cationic zinc(II) phthalocyanine Pc13 has shown to be a potent photosensitizer in different melanoma cell lines. In this study, we explored the intracellular signaling pathways triggered by Pc13 PDT and the role of these cascades in the phototoxic action of Pc13 in human melanoma A375 cells. ROS-dependent activation of MAPKs p38, ERK, JNK and PI3K-I/AKT was observed after treatment. Inhibition of p38 reduced Pc13 phototoxicity, whereas blockage of ERK did not affect this response. Conversely, JNK inhibition potentiated the effect of Pc13 PDT. Results obtained indicate that p38 is involved in the cleavage of PARP-1, an important mediator of apoptosis. On the other hand, Pc13 irradiation induced the activation of an autophagic program, as evidenced by enhanced levels of Beclin-1, LC3-II and GFP-LC3 punctate staining. We also demonstrated that this autophagic response is promoted by JNK and negatively regulated by PI3K-I/AKT pathway. The blockage of autophagy increased Pc13 phototoxicity and enhanced PARP-1 cleavage, revealing a protective role of this mechanism, which tends to prevent apoptotic cell death. Furthermore, reduced susceptibility to treatment and increased activation of autophagy were detected in A375 cells submitted to repeated cycles of Pc13 PDT, indicating that autophagy could represent a mechanism of resistance to PDT. The efficacy of Pc13 PDT and an improved phototoxic action in combination with chloroquine were also demonstrated in tumor spheroids. In conclusion, we showed the interplay between apoptotic and autophagic signaling pathways triggered by Pc13 PDT-induced oxidative

stress. Thus, autophagy modulation represents a promising therapeutic strategy to potentiate the efficacy of PDT in melanoma.

1. Introduction

Melanoma is a malignant and highly invasive skin carcinoma originated in melanocytes that represents the principal cause of cell death due to skin cancer. A recent study of the International Agency for Research on Cancer (IARC) of the World Health Organization (WHO) reported 287,723 new cases of melanoma worldwide in 2018 [1]. Although immunotherapy and targeted therapies have shown increased overall survival and progression-free survival of patients with melanoma, durable responses only occur in some patients, and those who initially respond can ultimately develop resistance after continued treatment [2]. Since the incidence of melanoma has notably increased in the last decade and given its intrinsic resistance to available therapies, new therapeutic alternatives need to be explored.

Photodynamic therapy (PDT) is a minimally invasive therapeutic procedure that combines the use of a non-toxic photosensitizer (PS) and visible light in order to exert a selective cytotoxic activity toward malignant cells. Irradiation at a wavelength corresponding to an absorbance band of the PS produces its excitation, which in the process of deactivation generates reactive oxygen species (ROS) by two main mechanisms, known as type I and type II reactions [3,4]. A type I process occurs when PS reacts directly with an organic molecule in a cellular microenvironment to form radicals and cytotoxic species, such as superoxide anion, hydrogen peroxide and hydroxyl radicals. In type II reactions, PS transfers its energy to molecular oxygen, leading to the formation of singlet oxygen ($^1O_2$), a highly cytotoxic molecule [5].

Accumulation of ROS leads to oxidative stress, a condition in which cellular constituents, including proteins, DNA and lipids are oxidized and damaged [6]. Host survival depends on the ability of cells to adapt to or resist the stress, and repair or remove damaged molecules. Numerous stress response mechanisms are rapidly

activated in response to oxidative insults, including non-enzymatic and enzymatic antioxidizing agents [7,8]. In addition, ROS activate different intracellular signaling pathways and can elicit a wide spectrum of responses, such as proliferation, growth arrest, senescence and cell death [9]. The response depends on the cell type, the stimulus examined, its dose and duration [10]. Mitogen-activated protein kinases (MAPKs) are a large number of serine/threonine kinases that can be activated in response to oxidant injury. MAPKs are divided into three multimember subfamilies: the extracellular signal-regulated kinases (ERK), the c-Jun N-terminal kinases (JNK), and the p38 kinases [11,12]. Phosphoinositide 3-kinase (PI3K) pathway is also regulated by ROS [13,14]. PI3K catalyzes the synthesis of the second messenger phosphatidylinositol 3,4,5 triphosphate (PIP3) from phosphatidylinositol 4,5 bisphosphate (PIP2). In the membrane, PIP3 recruits proteins such as the phosphoinositide dependent protein kinase (PDK) and protein kinase B (AKT), which are activated and mediate further downstream signaling events [15]. It was proposed that ROS may activate MAPK and PI3K pathways through the oxidative modification of intracellular kinases [9,16].

The increase of ROS can also trigger autophagy, an essential process that consists of selective degradation of cellular components. Under stress conditions autophagy has a pro-survival role involved in the turnover of proteins and elimination of damaged or aged organelles and cytoplasmic components to maintain cell homeostasis [17,18]. However, extensive autophagy or inappropriate activation of autophagy may be deleterious and lead to cell death [19–21]. In addition, the induction of an autophagic response has been demonstrated after photodynamic treatment, but dual roles of this process have been described, since it may induce either a survival response or contribute to a death pathway [22–24].

MAPKs and PI3K/AKT pathways have been associated with both apoptotic and autophagic responses [25–28]. Although activation of ERK, JNK and p38 has been reported in PDT-treated cells, the roles of these signaling pathways depend on the cell line and/or photosensitizer used [22,29–31]. In a previous work we demonstrated that the cationic zinc(II) phthalocyanine 2,9(10),16(17),23(24)-tetrakis[(2-trimethylammonium)ethylsulfanyl]phthalocyaninatozinc(II) tetraiodide (Pc13) (Fig. 1A) is a potent photosensitizer in a wide range of melanoma cell lines. The irradiation of Pc13 in melanoma cells simultaneously activates apoptotic and necrotic mechanisms, and the extent of cell death by necrosis can be modulated by Pc13 concentration and/or the light dose employed [32]. The aim of the present work is to explore the intracellular signaling pathways induced by Pc13 PDT in melanoma cells and the participation of these cascades in the phototoxic mechanism of Pc13. Results obtained demonstrated that the photodynamic treatment induced a ROS-dependent activation of MAPKs p38, JNK and ERK, and PI3K/AKT. Moreover, pro-survival autophagy was triggered after Pc13 PDT and this mechanism was increased in resistant cells submitted to repeated cycles of PDT. Inhibition of autophagy potentiated apoptotic cell death, demonstrating the interplay between both mechanisms in the photodynamic effect of Pc13 in melanoma cells. We also demonstrated the efficacy of Pc13 PDT and a potentiated phototoxicity of the combination with the autophagy inhibitor chloroquine in three-dimensional (3D) cellular aggregates. The study of the signaling pathways triggered by a potent second generation photosensitizer and the crosstalk between cell death and pro-survival mechanisms emphasizes the clinical relevance of combined therapies for melanoma treatment.

2. Materials and methods

2.1. Chemicals

Synthesis and purification of the sulfur-linked cationic 2,9(10),16(17),23(24)-tetrakis[(2-trimethylammonium)ethylsulfanyl]phthalocyaninatozinc(II) tetraioidide, named Pc13, has been previously described [33]. The antioxidant 6-hydroxy-2,5,7,8-tetramethylchroman-2-carboxylic acid (trolox) was from Sigma Chemical (St. Louis, MO). The p38 inhibitor SB 203580 was obtained from Santa Cruz Biotechnology (CA, USA). The JNK1/2 inhibitor SP 600125 was from Cayman Chemical Company (MI, USA) and the MEK inhibitor PD 98059 was from Promega (WI, USA). Autophagy inhibitors employed were wortmannin (WM) (Calbiochem, Darmstadt, Germany), 3-methyladenine (3-MA) (Santa Cruz Biotechnology, CA, USA) and chloroquine (CQ) (Sigma-Aldrich, MO, USA). Lipofectamine 3000 was provided by Thermo Fisher Scientific (MA, USA).

2.2. Antibodies

Monoclonal antibodies against phospho-p38 (p-p38), ERK1/2, phospho-JNK1/2 (p-JNK1/2), phospho-c-Jun (p-c-Jun), Bcl-2, LC3-II, Beclin-1, PARP-1, and the polyclonal antibody anti-p38 were obtained from Santa Cruz Biotechnology (CA, USA). Polyclonal antibodies directed to phospho-ERK1/2 (p-ERK1/2), phospho-AKT (p-AKT), and JNK1/2, and monoclonal antibodies against AKT and phospho-p90 (p-p90) were from Cell Signaling Technology (MA, USA). Monoclonal antibody against α-tubulin was purchased from Abcam (UK). Secondary antibodies anti-mouse IgG (horseradish peroxidase-conjugated goat IgG) or anti-rabbit IgG (horseradish peroxidase-conjugated goat IgG) were from Santa Cruz Biotechnology (CA, USA).

2.3. Plasmids

Dominant negative of p38 (DN p38), pcDNA3 p38α T180A/Y182F (Addgene plasmid #20352), and dominant negative of JNK1 (DN JNK1), pCDNA3 Flag JNK1-APF (Addgene plasmid #13846), were gifts from Dr. Roger Davis (University of Massachusetts Medical School, Worcester, MA, USA). The dominant negative mutant of the PI3K-I regulatory subunit p85 (DN PI3K-I), pWZL-neo δp85 del478-513 (Addgene plasmid #10888), was provided by Dr. William Hahn (Harvard Medical School, Boston, MA, USA). Dominant negative constructs of ERK1 and ERK2 (DN ERK1/2), pCEP4-ERK1-K71R and pCEP4-ERK2-K52R (Addgene plasmids #49329 and #39224), were gifts from Dr. Melanie Cobb (University of Texas Southwest Medical Center, Dallas, TX, USA). pEGFP-mRFP-LC3 plasmid (Addgene plasmid #21074) was kindly provided by Professor Tamotsu Yoshimori (Osaka University, Japan).

2.4. Cell culture

Human melanoma A375 cells (ATCC CRL-1619) were grown in DMEM F-12 medium with 10% (v/v) FBS (Natocor, Argentina), 2 mM L-glutamine, 50 U/ml penicillin, 50 μg/ml streptomycin (Sigma-Aldrich, MO, USA) and 4 mM sodium bicarbonate, in a humidified atmosphere of 5% CO_2 at 37ºC.

2.5. Photodynamic treatment

A375 cells grown until ~ 70% confluence were incubated with different concentrations of Pc13 in culture medium containing 4% FBS. After 16 h of incubation, cells were washed and complete fresh culture medium was added. Then, cells were maintained in

the dark or irradiated with a 150 W halogen lamp, equipped with a 10 mm water filter to attenuate IR radiation and a 630 nm cut-off filter. A 675 ± 15 nm bandpass filter (CVI Melles Griot, Albuquerque, USA) was employed to obtain power output at wavelengths to which there is maximum Pc13 absorbance. The total power output was 0.28 mW cm^{-2}, measured with a FieldMate laser power meter (Coherent, Wilsonville, USA) and the light dose at 675 ± 15 nm was 340 mJ cm^{-2} corresponding to 20 min of irradiation. In parallel, cells incubated in the absence of Pc13 were used as control.

When the effect of inhibitors was evaluated, A375 cells were incubated for 16 h with a solution of Pc13 corresponding to its IC_{50} value (3.60 μM). After washing with PBS, cells were pre-incubated for 1 h with 5 mM of the antioxidant trolox, 10 μM SB 203580, 10 μM SP 600125, 20 μM PD 98059, 0.5 μM wortmannin, 5 mM 3-MA or 20 μM chloroquine and then irradiated. Phototoxicity was evaluated following 24 h of incubation by colorimetric determination of hexosaminidase activity with p-nitrophenol substrate as previously described [34]. Absorbance values were measured in a Biotrack II Microplate Reader (GE Healthcare, Piscataway, NY).

2.6. Transfections

A375 cells grown at 70-80% confluence in 6 well-plates were transiently transfected with DN p38, DN PI3K-I, DN JNK1, DN ERK1/2 or the corresponding empty vectors (2.5 μg/well) using Lipofectamine 3000 reagent, according to the manufacturer's protocol. After overnight incubation, cells were employed for Western blot analysis or plated at a density of $1.5x10^4$/well in 96-well microplates and then incubated with IC_{50} Pc13 in culture medium containing 4% FBS for 24 h. After washing with PBS, cells were irradiated with a light dose of 340 mJ cm^{-2} and then incubated 24 h before cell growth determination by hexosaminidase method.

2.7. Western blot assays

A375 cells (2×10^6) were incubated overnight with 3.60 μM (IC_{50}) Pc13, then washed with PBS and exposed to a light dose of 340 mJ cm^{-2}. At different times post irradiation (p.i.), cells were lysed for 30 min at 4°C in 10 μl of lysis buffer (0.5% Triton X-100, 1 μg/ml aprotinin, 1 μg/ml trypsin inhibitor, 1 μg/ml leupeptin, 10 mM $Na_4P_2O_7$, 10 mM NaF, 1 mM Na_3VO_4, 1 mM EDTA, 1 mM PMSF, 150 mM NaCl, 50 mM Tris, pH 7.4). Clear supernatants were centrifuged at 17,000×*g* for 10 min at 4°C and protein concentration was determined using Bradford reagent. Aliquots containing 50 μg of protein were resuspended in 0.063 M Tris/HCl, pH 6.8, 2% SDS, 10% glycerol, 0.05% bromophenol blue, 5% 2-mercaptoethanol, submitted to SDS-PAGE and then transferred to PVDF membranes (GE Healthcare, Piscataway, NY) for 1 h at 100 mA per membrane (constant current) using the V20-SDB semi-dry blotting system (Scie-Plas, Cambridge, UK) in 25 mM Tris, 195 mM glycine, 20% methanol, 0.03% SDS, pH 8.2. To reduce non-specific binding, membranes were incubated for 1 h at room temperature in 10 mM Tris–HCl, 130 mM NaCl and 0.05% Tween 20, pH 7.4, (TBS-T), containing 5% non-fat milk. Membranes were then incubated overnight at 4°C with the primary antibody, washed with TBS-T and incubated with the corresponding secondary antibody conjugated with HRP for 1 h at room temperature. Immunoreactive proteins were visualized using the ECL Plus detection system (Pierce, Thermo Scientific, Rockford, USA) according to the manufacturer´s instructions. For quantification of band intensity, membranes were scanned using a densitometer (ImageQuant LAS 500, GE Healthcare Life Sciences). Equal protein loading was confirmed using a mouse anti-α-tubulin antibody or antibodies against the

corresponding non-phosphorylated proteins. Band intensities were quantified using Gel-Pro Analyzer 4.1 software (Media Cybernetics).

2.8. Generation of Pc13 PDT resistant cells

A375 cells cultured in 25 cm^2 flasks and incubated with Pc13 3.60 µM for 24 h, were exposed to a light dose of 680 mJ cm^{-2} (40 min of irradiation). When surviving cells proliferated, they were submitted to a new PDT treatment [35]. Cell populations that received a total of 5 or 10 cycles of Pc13 PDT were obtained and named $A375_{5\ PDT}$ and $A375_{10\ PDT}$, respectively. Resistant cells were maintained in frozen stocks. Susceptibility to Pc13 PDT was evaluated by hexosaminidase method. These cells were also employed for Western blot analysis.

2.9. GFP-LC3 overexpression and autophagy detection

A375 cells grown on coverslips at a density of $6x10^4$ cells/well in 24-well plates were transfected with pEGFP-mRFP-LC3 plasmid (0.5 µg/well) using Lipofectamine 3000, according to manufacturer's recommendations. Then, cells were incubated with IC_{50} Pc13 in medium containing 4% FBS for 24 h. After washing with PBS, cells were irradiated with a light dose of 340 mJ cm^{-2} and microphotographs of GFP-LC3 fluorescence were obtained with a Leica DM2000 fluorescence microscope at 470-490 nm excitation and 515 nm emission wavelengths at 1 h post-irradiation. Detection of punctated green staining of GFP-LC3 indicated the formation of autophagosomes.

Alternatively, transfections were also performed on A375, $A375_{5\ PDT}$ and $A375_{10\ PDT}$ without being submitted to light exposure.

2.10. Formation of 3D tumor spheroids and phototoxicity assay

A375 spheroids were generated by the liquid overlay technique [36]. Briefly, A375 cells were plated at a density of 2×10^3 cells/well in U shaped 96-well microplates pre-coated with sterile 1% agarose. The formation of spheroids was monitored by optical microscopy and spheroids' area was measured using Image J software. Spheroids reached a diameter of 400-500 μm at 3 days of culture. In order to evaluate Pc13 phototoxicity, spheroids were incubated with different concentrations of Pc13 in culture medium containing 4% FBS. After 24 h, the compound was removed and spheroids were exposed to a light dose of 680 mJ cm^{-2}. Spheroid areas were determined at different times post irradiation during 10 days. In parallel, non treated spheroids were used as control.

To evaluate spheroid viability, 12 spheroids from each condition were washed twice with PBS. Then, spheroids were disaggregated by incubation with trypsin 0.25%, EDTA 1mM for 10 min at 37°C. After neutralizing trypsin with complete growth medium, cells were resuspended and incubated with MTT (0.5 mg/ml) for 4 h. Formazan crystals were obtained by centrifugation at 400 x g and solubilized with isopropanol, HCl 0.04 N. Absorbance values at 595 nm were measured in a Biotrack II Microplate Reader (GE Healthcare, Piscataway, NY).

2.11. Statistical analysis

All data was presented and analyzed using GraphPad Prism (Version 6.01, GraphPad Software, La Jolla, California, USA, www.graphpad.com). Statistical analyses were performed by Student´s *t*-test (comparing two groups) or One-Way Anova with Dunnett post-test (comparing all groups to a control group). Differences in values were considered as statistically significant if p-value was less than 0.05 ($p<0.05$). All

experiments were conducted at least 3 times and expressed as mean ± SEM, unless otherwise indicated.

3. Results

3.1. ROS-mediated signaling pathways triggered by Pc13 PDT in A375 cells

In order to evaluate the susceptibility of human melanoma A375 cells to Pc13 PDT, cells were incubated in the presence of different concentrations of Pc13 and then irradiated with a light dose of 340 mJ cm^{-2}. As it is expected for all photosensitizers employed in PDT, cell viability was not affected in the dark, but a dose-dependent phototoxicity of Pc13 was observed after irradiation, being the concentration that caused 50% of cell death (IC_{50}) of 3.60 ± 0.23 μM (Fig. 1B). When cells were preincubated with the antioxidant trolox, the phototoxic effect of Pc13 was blocked, demonstrating that ROS are critical mediators of the photodynamic response.

Since both MAPKs and PI3K/AKT have been identified as signaling pathways involved in cellular oxidative stress response, the possible induction of these cascades in Pc13 PDT was studied. As shown in Fig. 2A, phosphorylation levels of MAPKs p38, ERK1/2 and JNK1/2 increased after phototreatment. While p38 and ERK were activated immediately after 20 min of irradiation (time 0 p.i.), the kinetic of JNK activation was slower. In addition, a time-dependent phosphorylation of AKT was observed with a maximum at 60 min p.i. Based on these findings, the role of ROS in the activation of these pathways in A375 cells was studied. In this regard, phosphorylation levels at the maximum time of activation for each MAPK and AKT were markedly reduced in the presence of 5 mM trolox (Fig. 2B).

3.2. Role of MAPKs and AKT in Pc13 phototoxicity

Since activation of MAPKs and PI3K-I/AKT pathways were related to both proliferation and cell death responses, we next explored the contribution of these cascades in Pc13 response. For this purpose, A375 cells were exposed to IC_{50} of Pc13

and irradiated in the presence of specific inhibitors. Cell viability significantly increased when cells were preincubated with p38 inhibitor SB 203580, whereas SP 600125, a JNK1/2 inhibitor potentiated Pc13 phototoxicity (Fig. 3A). No changes in cell viability were observed in the presence of MEK inhibitor PD 98059. Similar studies were performed in cells transfected with dominant negative mutants for p38, JNK1 and ERK1/2. Transfection efficiency was verified by a reduction in the level of p-p38, p-cJun or p-p90, respectively (Supplementary Fig. 1). As it was observed with p38 inhibitor, transfection with DN p38 also reduced Pc13 phototoxicity, suggesting that this pathway is involved in cell death. On the other hand, DN JNK1 overexpression led to increased Pc13 phototoxicity, whereas no changes were observed with DN ERK1/2. Finally, transfection with a dominant negative of PI3K-I reduced both AKT phosphorylation (Supplementary Fig. 1) and Pc13 phototoxic action (Fig. 3B).

Since Pc13 phototoxicity was reduced when p38 was inhibited, we then explored whether this kinase plays a role in Pc13 PDT-induced apoptosis. In this sense, we have previously demonstrated that photodynamic treatment with Pc13 induces a dual apoptotic and necrotic response in melanoma cells [32]. The cleavage of PARP-1, a marker of apoptosis, was demonstrated after irradiation of Pc13-loaded A375 cells (Fig. 3C). When cells where preincubated with the inhibitor of p38 SB 203580, a significant decrease in the level of the 89 kDa fragment of PARP-1 was observed, suggesting that p38 activation is involved in the apoptotic cell death triggered by Pc13 PDT.

3.3. Pc13 photoactivation induces protective autophagy in A375 cells

Although it has been previously reported that PDT can trigger autophagy, its role in cell death is ambiguous. In order to study the involvement of this mechanism in Pc13 phototoxicity, we investigated the conversion of microtubule-associated protein light

chain 3 (LC3-I) to LC3-II. During autophagy, cytosolic LC3-I is conjugated to phosphatidylethanolamine and lipidated LC3-II translocates to the autophagosome membrane [37]. The amount of LC3-II is closely correlated with autophagosomes formation and it is commonly employed as an autophagy indicator. As shown in Fig. 4A, an increase in LC3-II levels was observed 30 and 60 min after irradiation. Moreover, Pc13 PDT dramatically induced green fluorescence shift from a diffuse to a punctate pattern in A375 cells transfected with LC3-GFP plasmid (Fig. 4B), indicating that cytosolic LC3 was translocated to autophagosomes. A marked increase of Beclin-1, another regulator of autophagosome formation, was detected after irradiation of Pc13-treated cells (Fig. 4C). It was reported that BH3 domain of Beclin-1 is bound to, and inhibited by Bcl-2 or Bcl-XL [38,39]. Interestingly, we observed a reduction in the expression levels of Bcl-2 after treatment, suggesting that Beclin-1 would be free to promote autophagosome formation (Fig. 4C).

Then, we examined the role of autophagy activation in Pc13 phototoxicity. When different inhibitors of autophagy, including chloroquine (CQ) and the PI3K inhibitors 3-methyladenine (3-MA) and wortmannin (WM), were employed in combination with Pc13 PDT, an enhanced phototoxicity was observed (Fig. 4D). Taken together, these results indicate that that autophagy triggered by Pc13 PDT promotes cell survival in A375 cells.

3.4. JNK and PI3K-I/AKT regulate Pc13 PDT-induced autophagy

In order to study the participation of MAPKs in the autophagic response induced by irradiation of Pc13 in A375 cells, we used pharmacologic inhibitors of p38 and JNK, the kinases that were involved in the phototoxic action of Pc13 (Fig. 3A). As it is shown in Fig. 5, while SB 203580 had no effect on the conversion of LC3, the expression of

LC3-II was significantly downregulated by SP 600125 in Pc13 PDT treated cells, suggesting that JNK activation participates in the induction of autophagy. On the other hand, since PI3K inhibitors affect both class I and class III PI3K, we employed a dominant negative of PI3K-I to specifically block this pathway. Under this condition, the levels of LC3-II were significantly higher than in non transfected cells after Pc13 PDT (Fig. 5), demonstrating that activation of PI3K-I/AKT pathway inhibits autophagy. Thus, JNK and PI3K-I/AKT signaling pathways have opposite roles in the autophagy triggered by Pc13 photoactivation. While JNK promotes the conversion of LC3 involved in autophagosome formation and protects cells from death, PI3K-I/AKT blocks this mechanism and increase sensitivity to photodynamic treatment.

3.5. Autophagy is increased in melanoma cells resistant to PDT

Results obtained demonstrate that autophagy induced by Pc13 PDT has a protective role in response to oxidative stress. Therefore, we decided to evaluate whether repeated cycles of PDT on melanoma cells could affect the phototoxic outcome through changes in the autophagic response. Thus, A375 cells were exposed to 3,60 µM of Pc13 and irradiated with a light dose of 680 mJ cm^{-2}. Then, surviving cells were submitted to additional four or nine cycles of PDT treatments, leading to $A375_{5\ PDT}$ and $A375_{10\ PDT}$ cells, respectively (Fig. 6A). As it is shown in Figure 6B, IC_{50} values in $A375_{5\ PDT}$ and $A375_{10\ PDT}$ cells were 6-7 times higher than in parental A375 cells. Furthermore, increased levels of LC3-II and a more punctate staining of GFP-LC3 were observed in cells that received repeated cycles of PDT (Fig. 6C and 6D). These results demonstrate that autophagy is over-stimulated after several photodynamic treatments and this produces a reduction in the phototoxic sensitivity.

3.6. Inhibition of autophagy increases the PDT apoptotic response and potentiates Pc13 phototoxicity in 3D tumor spheroids

Since Pc13 PDT can trigger both apoptotic and protective autophagic responses, the final fate of a cell after irradiation will depend on the balance between cell death and prosurvival mechanisms. To evaluate the crosstalk between apoptotic and autophagic pathways, cells were incubated with the autophagy inhibitor chloroquine and submitted to phototreatment. Western blot analysis revealed that inhibition of autophagy by 20 μM chloroquine enhanced Pc13 PDT-induced cleavage of PARP-1 (Fig. 7). Thus, an increased induction of apoptosis was obtained when autophagy was blocked, demonstrating the interplay between both mechanisms, in which autophagy negatively regulates apoptosis in Pc13 phototoxic response.

The photodynamic effect of Pc13 was subsequently evaluated in 3D culture models. After formation, A375 spheroids were exposed to different concentrations of Pc13 and irradiated with a light dose of 680 mJ cm^{-2}. Spheroid images obtained by optical microscopy were employed to determine areas at different times post irradiation. As shown in Fig. 8A, PDT caused a decrease in spheroid growth in a dose dependent manner, being 10 μM Pc13 the concentration that produced the maximum effect. The reduction of spheroid area correlated with a decrease in cell viability, as determined by MTT assay (Fig. supplementary 2).

When a suboptimal concentration of Pc13 (2.5 μM) was employed, the addition of chloroquine potentiated the reduction of spheroid growth, demonstrating that autophagy is a protective mechanism that counteracts the phototoxic efficacy of Pc13 in 3D models, as it was shown in 2D cultures (Fig. 8B).

4. Discussion

Photodynamic therapy is a treatment modality that involves the production of ROS, leading to oxidative stress in the irradiated cells. ROS are critical signaling molecules involved in a wide variety of cellular processes, such as apoptosis, cell proliferation and survival [9]. We have previously demonstrated the ROS-mediated phototoxic effect of the zinc phthalocyanine Pc13 in different melanoma cells [32]. In the present work, we explored the signaling pathways activated and the intracellular mechanisms triggered by Pc13 PDT. We showed that irradiation of human A375 melanoma cells treated with Pc13 induced the activation of MAPKs p38, JNK and ERK, and PI3K-I/AKT pathways (Fig. 9). Among MAPK cascades, the apoptosis signal-regulated kinase 1 (ASK1) is an upstream kinase that regulates MAPK pathways and can be activated under oxidative stress [11,40]. While ASK1 is inhibited by reduced thioredoxin in nonstressed cells, it is activated when two cysteine residues of thioredoxin are oxidized, leading to dissociation of thioredoxin from ASK1, resulting in the activation of JNK and p38 pathways [41]. It was also proposed that MAPK pathways can also be activated by the direct inhibition of MAPK phosphatases by ROS [42]. Similarly, the PI3K pathway is subject to reversible redox regulation by ROS. This pathway is negatively regulated by the phosphatase and tensin homology (PTEN). It was demonstrated that ROS oxidize and inactivate PTEN, causing the activation of the PI3K pathway [14]. When A375 cells were submitted to PDT in the presence of the antioxidant trolox, p38, JNK, ERK and AKT phosphorylation was prevented, indicating that oxidative stress triggered by Pc13 PDT is responsible for MAPKs and PI3K-I/AKT pathways activation.

In the context of PDT, MAPKs and PI3K pathways have been related to both survival and cell death, depending on the tumor cell type, the stimulus duration and the photosensitizer employed [22,29,30]. Thus, we studied the role of these intracellular

pathways in the phototoxicity of Pc13 in A375 cells. Results obtained demonstrated that p38 is involved in the apoptotic cell death triggered by irradiation of Pc13-treated cells (Fig. 9). Accordingly, Xue *et al.* observed p38 activation in the apoptotic response of PDT employing the phthalocyanine Pc 4 in CHO cells [43]. In a recent work, the siRNA targeting of p38 was used to reveal the mitochondria-mediated apoptosis in ZnPc PDT-treated colon carcinoma LoVo cells [44]. On the other hand, we showed that while inhibition of ERK had no considerable effect, the blockage of JNK with a specific inhibitor or with over-expression of a dominant negative mutant potentiated the phototoxic effect of Pc13, suggesting that JNK participates in cell survival.

Since autophagy was reported to be involved in both cell death and survival in response to oxidative stress [6], the activation of this mechanism after Pc13 PDT was herein studied. We found different evidence of autophagy induction, including increase of Beclin-1, the conversion of LC3-I to LC3-II and accumulation of LC3 in autophagosome vesicles after PDT. While some works proposed a pro-death role of PDT-induced autophagy [22,23,45], other reports suggested that it plays a protective role [46,47]. It's worthy to mention that autophagy triggers cell death in apoptosis incompetent cells [48]. In this work, we showed that the inhibition of autophagy resulted in an increased Pc13 phototoxicity, indicating that Pc13 PDT-triggered autophagy mediates cell survival.

Autophagy is regulated by different isoforms of PI3K in opposite manner. While PI3K-I/AKT signaling pathway blocks the promotion of autophagy via the activation of mTOR, a class III PI3K complex, formed with Beclin-1, class III PI3K, and p150, recruits LC3 to the membrane of autophagosomes and thereby activates autophagy[49]. Since PI3K inhibitors affect both class I and class III PI3K [50], we employed a dominant negative of PI3K-I to specifically block AKT cascade. This blockage

increased the induction of autophagy and reduced Pc13 phototoxicity, indicating that PI3K-I/AKT pathway activated by Pc13 PDT inhibits the induction of a protective autophagy. In this sense, Espada *et al.* reported that the constitutive activation of H-Ras or PI3K-I, associated with AKT phosphorylation, is sufficient to protect murine keratinocytes from PDT using a Zn phthalocyanine as photosensitizer, indicating that this signaling pathway plays a key role in cell survival [51]. Conversely, PI3K inhibitors, such as wortmannin and 3-MA, usually employed as autophagy inhibitors, increased phototoxic effect of Pc13. Chloroquine, by a different mechanism of autophagy inhibition, also increased cell death after PDT. The raise of lysosomal pH caused by chloroquine leads to inhibition of both fusion of autophagosome with lysosome and lysosomal protein degradation. Taking into account that autophagy contributes to cell survival after photodynamic treatment with Pc13, we further evaluated if this mechanism was exacerbated in A375 cells submitted to several cycles of Pc13 PDT. Results obtained demonstrated a significant reduction in sensitivity to treatment together with an increase in LC3-II levels in A375 $_{5\ PDT}$ and A375 $_{10\ PDT}$ cells, suggesting that autophagy is a mechanism involved in PDT resistance. Accordingly, Martin *et al.* identified an autophagic response in vemurafenib-resistant melanoma cells [52]. Similarly, Rodríguez *et al.* found that hypoxia activates a HIF-1α/VMP1 autophagy pathway that confers resistance to PDT in colon cancer cells [46].

The efficacy of PDT treatment with Pc13 was further demonstrated in 3D cultures of A375 cells. It was reported that gene expression profiles of tumor spheroids are more similar to in vivo gene expression than those in 2D culture [53]. Furthermore, since tumor spheroids resemble the hypoxic condition and cell-cell interactions of in vivo tumors, in general they have reduced responsiveness to treatments. We showed that the combination of Pc13 PDT with chloroquine was more phototoxic than PDT

alone. In a recent work, Yu *et al.* also demonstrated that PDT with an unsubstituted ZnPc and 3-MA inhibited tumor growth, indicating that autophagy indeed exerts a protective role [54].

Results obtained demonstrated that Pc13-activated JNK has a positive regulation in LC3-II formation, since incubation with SP 600125 significantly reduced the expression level of LC3-II. In this sense, it was reported that JNK1 mediates the phosphorylation of Bcl-2, an inhibitor of Beclin-1, leading to disruption of Bcl-2-Beclin-1 interaction and autophagy induction [38]. After Pc13 PDT we observed not only an increase in Beclin-1, but also a reduction in Bcl-2 levels that may promote autophagosome formation. Diminished levels of Bcl-2 are also related to the induction of apoptotic cell death after PDT [32]. Thus, the anti-apoptotic protein Bcl-2 regulates both apoptosis and cell survival by autophagy. In order to confirm the interplay between these mechanisms in PDT response, we evaluated the apoptotic response in the presence of chloroquine. We proved that autophagy inhibition enhances the apoptotic outcome, as evidenced by an augmented cleavage of PARP-1. The crosstalk between apoptosis and autophagy was previously demonstrated by different approaches. It was shown that ABT737, a BH3 domain mimetic that competitively inhibits the interaction between Beclin-1 and Bcl-2, antagonized autophagy inhibition by Bcl-2, stimulating autophagy [55]. In the same way, Beclin-1 mutants that cannot bind to Bcl-2 induce more autophagy than wild-type Beclin-1 [56]. In addition, caspases, activated during apoptosis, can cleave Beclin-1, thereby blocking its pro-autophagic activity [57,58]. On the other hand, Beclin-1 can act as an anti-apoptotic protein under different situations, including chemotherapy, irradiation, immunotherapy, nutrient deprivation, angiogenesis inhibitors and hypoxia [39].

In conclusion, in this work we provide evidence that photodynamic therapy with Pc13 is an efficient antitumor modality for melanoma treatment that induces oxidative stress, responsible for the activation of MAPKs and PI3K-I/AKT pathways. These signaling cascades are involved in the induction of an apoptotic response, but also in triggering protective autophagy. While p38 pathway mediates apoptosis, JNK and PI3K-I/AKT inversely regulate autophagy (Fig 9). Therefore, the final fate of Pc13 PDT-treated cells depends on the balance between pro-death and pro-survival mechanisms activated in response to the oxidative insult. Thus, the identification of an apoptotic-autophagic interplay points out that autophagy blockage is a potential target to obtain an enhanced PDT antitumor efficacy for melanoma treatment.

Acknowledgements

This work was supported by grants of Agencia Nacional de Promoción Científica y Tecnológica PICT 2013-0144, Consejo Nacional de Investigaciones Científicas y Técnicas PIP 0154 and Secretaría de Ciencia y Técnica de la Universidad de Buenos Aires (UBACyT 20020130100024), Argentina. Authors are grateful to Dr. Marcela Villaverde for the generous gift of A375 cells.

Conflict of interest

The authors declare that they have no conflict of interest.

Figure legends

Figure 1. Phototoxic effect of Pc13 on human melanoma A375 cells. A) Chemical structure of Pc13. B) A375 cells incubated with different concentrations of Pc13 for 24 h were pretreated or not with 5 mM of the antioxidant trolox, and then maintained in the dark or exposed to a light dose of 340 mJ cm^{-2}. Phototoxicity was evaluated 24 h after irradiation by hexosaminidase method. Results are expressed as the percentage of cell viability relative to control obtained in the absence of Pc13 and represent the mean ± SEM of three different experiments.

Figure 2. MAPKs and PI3K-I/AKT activation after Pc13 PDT. A) A375 cells treated with Pc13 3.60 μM were exposed to a light dose of 340 mJ cm^{-2} and incubated for different time-periods. B) Pc13-treated cells were incubated in the absence or presence of 5 mM Trolox for 1 h and then irradiated. Cells were harvested immediately after irradiation (time 0 p.i.) for p38 and ERK1/2 or 60 min p.i. for JNK1/2 and AKT analyses. Cell lysates (50 μg/lane) were submitted to Western blot assays. Representative experiments for p38, ERK1/2, JNK1/2 and AKT are shown. Band intensities were quantified using Gel-Pro Analyzer 4.1 software (Media Cybernetics). Results are expressed as the relation of phosphorylated to total kinase relative to control (irradiated cells without Pc13) and correspond to mean ± SEM of three different experiments. ANOVA-Dunnett *$p < 0.05$, **$p < 0.01$, significantly different from control.

Figure 3. Role of MAPKs p38, ERK, JNK and PI3K-I/AKT in the phototoxicity induced by Pc13. A) A375 cells incubated with Pc13 3.60 μM were pretreated or not with SB 203580 10 μM, SP 600125 10 μM or PD 98059 20 μM before irradiation with

a light dose of 340 mJ cm^{-2}. B) Alternatively, A375 cells transfected with DN p38, DN JNK1, DN ERK1/2, DN PI3K-I or the corresponding empty vectors were incubated with Pc13 3.60 μM and then irradiated. Cell viability was evaluated after 24 h of incubation by hexosaminidase method. C) Detection of cleaved PARP-1 (89 kDa fragment) by Western blot assay in lysates (50 μg/lane) of A375 cells submitted to Pc13 PDT in the absence or presence of SB 203580 10 μM. α-tubulin was used as loading control. Densitometric analyses were performed with Gel-Pro Analyzer software. Results represent the mean ± SEM, n= 3. ANOVA-Dunnett **$p < 0.01$, significantly different from Pc13 PDT-treated cells without inhibitors (A and C) or transfected with the corresponding empty vectors (B); ns, not significant.

Figure 4. Induction of autophagy by Pc13 photoactivation. A) A375 cells were treated with 3.60 μM Pc13 and irradiated with a light dose 340 mJ cm^{-2}. After incubating cells for the indicated times, total proteins were extracted and LC3-I/II was detected using Western blot analyses, in which α-tubulin served as a loading control. Results obtained by densitometric analyses are expressed as the ratio of LC3-II/tubulin relative to control (irradiated cells without Pc13). B) Following transfection with GFP-LC3 expressing vector, A375 cells were treated with 3.60 μM Pc13, irradiated with a light dose of 340 mJ cm^{-2}. At 1 h p.i., cells were examined using a fluorescence microscope. The appearance of punctate staining indicates autophagosome-associated LC3-II, scale bar 20 μm. C) Western blot of Beclin-1 and Bcl-2 at different times post irradiation of Pc13-treated A375 cells. D) A375 cells incubated with 3.60 μM Pc13 were pretreated with the autophagy inhibitors CQ 20 μM, 3-MA 5 mM or WM 0.5 μM, and irradiated with a light dose of 340 mJ cm^{-2}. Phototoxicity was evaluated 24 h after irradiation by hexosaminidase method. Results are expressed relative to control

obtained in the absence of Pc13 and represent the mean ± SEM, n= 3. ANOVA-Dunnett *p < 0.05, **p < 0.01, significantly different from control obtained in the absence of Pc13; ##p < 0.01, significantly different from Pc13 PDT-treated cells.

Figure 5. JNK and PI3K-I pathways regulate autophagy induced by Pc13 PDT. A375 cells treated with Pc13 3.60 μM were preincubated with SB 203580 10 μM, SP 600125 10 μM or transiently transfected with a DN PI3K-I vector before irradiation with a light dose of 340 mJ cm^{-2}. LC3-II levels were analyzed by Western blot assay of cell lysates obtained at 1 h p.i. and α-tubulin was employed as loading control. Results from one representative experiment are shown (upper panel). Densitometric analyses (lower panel) were performed with Gel-Pro Analyzer software. Results are expressed as the ratio of LC3-II/α-tubulin relative to control. ANOVA-Dunnett (n= 3) *p<0.05, **p < 0.01, significantly different from Pc13 PDT-treated A375 cells.

Figure 6. Autophagy is stimulated in resistant cells submitted to repeated cycles of Pc13 PDT. A) Schematic representation of Pc13 PDT resistant cells generation. B) A375 cells submitted to 5 or 10 cycles of PDT ($A375_{5\ PDT}$ and $A375_{10\ PDT}$) or parental A375 cells were incubated with different concentrations of Pc13 for 24 h and then exposed to a light dose of 340 mJ cm^{-2}. Phototoxicity was evaluated 24 h after irradiation by hexosaminidase method. Results are expressed as the percentage of cell viability relative to control obtained in the absence of Pc13 and represent the mean ± SEM of three different experiments. IC_{50} values, corresponding to the concentrations of Pc13 that produce 50% of cell death, are indicated. C) LC3-II levels in A375, $A375_{5\ PDT}$ and $A375_{10\ PDT}$ cells lysates were determined by Western blot assay. α-tubulin was used as loading control. Densitometric analyses were performed with Gel-Pro Analyzer

software. Results are expressed as the ratio of LC3-II/α-tubulin. ANOVA-Dunnett (n= 3) *p < 0.05; **p < 0.01, significantly different from A375 cells. D) A375, $A375_{5\ PDT}$ and $A375_{10\ PDT}$ cells were transiently transfected with GFP-LC3 expressing vector and then cell fluorescence was examined by fluorescence microscopy at 470-490 nm excitation and 515 nm emission wavelengths. Punctate staining indicates autophagosome-associated LC3-II. Scale bar 50 μm.

Figure 7. Blockage of autophagy enhances apoptotic response after Pc13 PDT. A375 cells treated with Pc13 3.60 μM were incubated for 1 h with CQ 20 μM and then irradiated with a light dose of 340 mJ cm^{-2}. Cell lysates obtained at 3 h post irradiation were submitted to Western blot assay for PARP-1 fragment (89 kDa) detection. α-tubulin was used as loading control. Results from one representative experiment are shown (upper panel). Densitometric analyses (lower panel) were performed with Gel-Pro Analyzer software. Results are expressed relative to control obtained in the absence of Pc13 and represent the mean ± SEM of three different experiments. Student´s *t*-test **p < 0.01.

Figure 8. Pc13-induced phototoxic effect on A375 spheroids. (A) A375 spheroids were incubated in the absence or presence of different concentrations of Pc13 (B) with or without chloroquine 20 μM and exposed to a light dose of 680 mJ cm^{-2}. Spheroid areas were determined at different days post irradiation using Image J software (upper panel). Results represent the mean ± S.D., n= 12, ANOVA-Dunnet *p < 0.05, **p < 0.01 significantly different from control spheroids incubated in the absence of Pc13, #p < 0.05, ##p < 0.01 significantly different from PDT treated-spheroids (Pc13 2.5 μM). Representative images of A375 spheroids are shown (lower panels). Scale bar 500 μm.

Figure 9. Signaling pathways triggered by Pc13 PDT in A375 melanoma cells. The irradiation of Pc13-loaded cells triggers the activation of ROS-mediated MAPKs p38, ERK, JNK and PI3K-I/AKT pathways. These pathways have different roles in the induction of apoptotic cell death and protective autophagy. While p38 mediates the apoptotic response, JNK promotes and PI3K-I/AKT pathway negatively regulates cell survival by autophagy. The balance between these mechanisms determines the final fate of the cell and modulates PDT efficacy.

Supplementary figure 1. Transfection of A375 cells with dominant negative mutants inhibits MAPKs and PI3K-I pathways. A375 cells transfected or not with DN p38, DN JNK1, DN ERK1/2 or DN PI3K-I were incubated in the absence or presence of Pc13 3.60 μM for 24 h. Then, cells were irradiated with a light dose of 340 mJ cm^{-2} and harvested immediately after irradiation (time 0 p.i.) or 60 min p.i. to evaluate p38 and ERK or JNK and PI3K-I pathway inhibition, respectively. Cell lysates (50 μg/lane) were submitted to Western blot assays. Representative blots of downstream targets of each kinases are shown: p-p38 (p38), p-p90 (ERK), p-cJun (JNK) and AKT (PI3K-I).

Supplementary figure 2. A375 spheroids viability decreased after Pc13 PDT. A375 spheroids incubated or not with different concentrations of Pc13 were exposed to a light dose of 680 mJ cm^{-2}. 10 days after irradiation, spheroids were disaggregated with trypsin and cell viability was determined by MTT reduction assay. Results are expressed as the percentage of cell viability relative to control obtained in the absence of Pc13 and represent the mean ± SEM of three different experiments.

References

[1] F. Bray, J. Ferlay, I. Soerjomataram, R.L. Siegel, L.A. Torre, A. Jemal, Global cancer statistics 2018: GLOBOCAN estimates of incidence and mortality worldwide for 36 cancers in 185 countries, CA. Cancer J. Clin. (2018). https://doi.org/10.3322/caac.21492.

[2] P. Sharma, S. Hu-Lieskovan, J.A. Wargo, A. Ribas, Primary, Adaptive, and Acquired Resistance to Cancer Immunotherapy, Cell. (2017). https://doi.org/10.1016/j.cell.2017.01.017.

[3] P. Agostinis, K. Berg, K.A. Cengel, T.H. Foster, A.W. Girotti, S.O. Gollnick, S.M. Hahn, M.R. Hamblin, A. Juzeniene, D. Kessel, M. Korbelik, J. Moan, P. Mroz, D. Nowis, J. Piette, B.C. Wilson, J. Golab, Photodynamic therapy of cancer: An update, CA. Cancer J. Clin. (2011). https://doi.org/10.3322/caac.20114.

[4] C.S. Oliveira, R. Turchiello, A.J. Kowaltowski, G.L. Indig, M.S. Baptista, Major determinants of photoinduced cell death: Subcellular localization versus photosensitization efficiency, Free Radic. Biol. Med. (2011). https://doi.org/10.1016/j.freeradbiomed.2011.05.023.

[5] K. Plaetzer, B. Krammer, J. Berlanda, F. Berr, T. Kiesslich, Photophysics and photochemistry of photodynamic therapy: Fundamental aspects, Lasers Med. Sci. (2009). https://doi.org/10.1007/s10103-008-0539-1.

[6] R. Scherz-Shouval, Z. Elazar, Regulation of autophagy by ROS: Physiology and pathology, Trends Biochem. Sci. (2011). https://doi.org/10.1016/j.tibs.2010.07.007.

[7] J. Dorval, A. Hontela, Role of glutathione redox cycle and catalase in defense against oxidative stress induced by endosulfan in adrenocortical cells of rainbow

trout (Oncorhynchus mykiss), Toxicol. Appl. Pharmacol. (2003). https://doi.org/10.1016/S0041-008X(03)00281-3.

[8] J.C. Kern, J.P. Kehrer, Free radicals and apoptosis: Relationships with glutathione, thioredoxin and the bcl family of proteins, Front. Biosci. (2005). https://doi.org/10.2741/1656.

[9] P.D. Ray, B.W. Huang, Y. Tsuji, Reactive oxygen species (ROS) homeostasis and redox regulation in cellular signaling, Cell. Signal. (2012). https://doi.org/10.1016/j.cellsig.2012.01.008.

[10] J.L. Martindale, N.J. Holbrook, Cellular response to oxidative stress: Signaling for suicide and survival, J. Cell. Physiol. (2002). https://doi.org/10.1002/jcp.10119.

[11] K. Tobiume, A. Matsuzawa, T. Takahashi, H. Nishitoh, K.I. Morita, K. Takeda, O. Minowa, K. Miyazono, T. Noda, H. Ichijo, ASK1 is required for sustained activations of JNK/p38 MAP kinases and apoptosis, EMBO Rep. (2001). https://doi.org/10.1093/embo-reports/kve046.

[12] M. Raman, W. Chen, M.H. Cobb, Differential regulation and properties of MAPKs, Oncogene. (2007). https://doi.org/10.1038/sj.onc.1210392.

[13] L.O. Klotz, S.M. Schieke, H. Sies, N.J. Holbrook, Peroxynitrite activates the phosphoinositide 3-kinase/Akt pathway in human skin primary fibroblasts, Biochem. J. (2000). https://doi.org/10.1042/0264-6021:3520219.

[14] J. Kwon, S.R. Lee, K.S. Yang, Y. Ahn, Y.J. Kim, E.R. Stadtman, S.G. Rhee, Reversible oxidation and inactivation of the tumor suppressor PTEN in cells stimulated with peptide growth factors, Proc. Natl. Acad. Sci. U. S. A. (2004). https://doi.org/10.1073/pnas.0407396101.

[15] D.A. Cantrell, Phosphoinositide 3-kinase signalling pathways, J. Cell Sci. (2001).

https://doi.org/10.1142/p428.

[16] Y. Son, Y.-K. Cheong, N.-H. Kim, H.-T. Chung, D.G. Kang, H.-O. Pae, Mitogen-Activated Protein Kinases and Reactive Oxygen Species: How Can ROS Activate MAPK Pathways?, J. Signal Transduct. (2011). https://doi.org/10.1155/2011/792639.

[17] B. Levine, D.J. Klionsky, Development by self-digestion: Molecular mechanisms and biological functions of autophagy, Dev. Cell. (2004). https://doi.org/10.1016/S1534-5807(04)00099-1.

[18] N. Mizushima, Autophagy: Process and function, Genes Dev. (2007). https://doi.org/10.1101/gad.1599207.

[19] M. Kundu, C.B. Thompson, Autophagy: Basic Principles and Relevance to Disease, Annu. Rev. Pathol. Mech. Dis. (2008). https://doi.org/10.1146/annurev.pathmechdis.2.010506.091842.

[20] C. Yang, V. Kaushal, S. V. Shah, G.P. Kaushal, Autophagy is associated with apoptosis in cisplatin injury to renal tubular epithelial cells, Am. J. Physiol. - Ren. Physiol. (2008). https://doi.org/10.1152/ajprenal.00590.2007.

[21] G. Kroemer, B. Levine, Autophagic cell death: The story of a misnomer, Nat. Rev. Mol. Cell Biol. (2008). https://doi.org/10.1038/nrm2529.

[22] E. Buytaert, M. Dewaele, P. Agostinis, Molecular effectors of multiple cell death pathways initiated by photodynamic therapy, Biochim. Biophys. Acta - Rev. Cancer. (2007). https://doi.org/10.1016/j.bbcan.2007.07.001.

[23] D. Kessel, N.L. Oleinick, Cell Death Pathways Associated with Photodynamic Therapy: An Update, Photochem. Photobiol. (2018). https://doi.org/10.1111/php.12857.

[24] L.P. Roguin, N. Chiarante, M.C. García Vior, J. Marino, Zinc(II)

phthalocyanines as photosensitizers for antitumor photodynamic therapy, Int. J. Biochem. Cell Biol. (2019). https://doi.org/10.1016/j.biocel.2019.105575.

[25] X. Sui, N. Kong, L. Ye, W. Han, J. Zhou, Q. Zhang, C. He, H. Pan, P38 and JNK MAPK pathways control the balance of apoptosis and autophagy in response to chemotherapeutic agents, Cancer Lett. (2014). https://doi.org/10.1016/j.canlet.2013.11.019.

[26] S.T. Pan, Y. Qin, Z.W. Zhou, Z.X. He, X. Zhang, T. Yang, Y.X. Yang, D. Wang, J.X. Qiu, S.F. Zhou, Plumbagin induces G2/M arrest, apoptosis, and autophagy via p38 MAPK- and PI3K/Akt/mTOR-mediated pathways in human tongue squamous cell carcinoma cells, Drug Des. Devel. Ther. (2015). https://doi.org/10.2147/DDDT.S76057.

[27] N.K. Niu, Z.L. Wang, S.T. Pan, H.Q. Ding, G.H.T. Au, Z.X. He, Z.W. Zhou, G. Xiao, Y.X. Yang, X. Zhang, T. Yang, X.W. Chen, J.X. Qiu, S.F. Zhou, Pro-apoptotic and pro-autophagic effects of the aurora kinase A inhibitor alisertib (MLN8237) on human osteosarcoma U-2 OS and MG-63 cells through the activation of mitochondria-mediated pathway and inhibition of p38 MAPK/PI3K/Akt/mTOR signaling pathway, Drug Des. Devel. Ther. (2015). https://doi.org/10.2147/DDDT.S74197.

[28] Y.Y. Zhou, Y. Li, W.Q. Jiang, L.F. Zhou, MAPK/JNK signalling: A potential autophagy regulation pathway, Biosci. Rep. (2015). https://doi.org/10.1042/BSR20140141.

[29] R.D. Almeida, B.J. Manadas, A.P. Carvalho, C.B. Duarte, Intracellular signaling mechanisms in photodynamic therapy, Biochim. Biophys. Acta - Rev. Cancer. (2004). https://doi.org/10.1016/j.bbcan.2004.05.003.

[30] H.T. Ji, L.T. Chien, Y.H. Lin, H.F. Chien, C.T. Chen, 5-ALA mediated

photodynamic therapy induces autophagic cell death via AMP-activated protein kinase, Mol. Cancer. (2010). https://doi.org/10.1186/1476-4598-9-91.

[31] X. Ge, J. Liu, Z. Shi, L. Jing, N. Yu, X. Zhang, Y. Jiao, Y. Wang, P. Andy Li, Inhibition of MAPK signaling pathways enhances cell death induced by 5-aminolevulinic acid-photodynamic therapy in skin squamous carcinoma cells, Eur. J. Dermatology. (2016). https://doi.org/10.1684/ejd.2015.2725.

[32] F. Valli, M.C. García Vior, L.P. Roguin, J. Marino, Oxidative stress generated by irradiation of a zinc(II) phthalocyanine induces a dual apoptotic and necrotic response in melanoma cells, Apoptosis. (2019). https://doi.org/10.1007/s10495-018-01512-w.

[33] J. Marino, M.C. García Vior, L.E. Dicelio, L.P. Roguin, J. Awruch, Photodynamic effects of isosteric water-soluble phthalocyanines on human nasopharynx KB carcinoma cells, Eur. J. Med. Chem. (2010). https://doi.org/10.1016/j.ejmech.2010.06.002.

[34] J. Marino, M.C. García Vior, V.A. Furmento, V.C. Blank, J. Awruch, L.P. Roguin, Lysosomal and mitochondrial permeabilization mediates zinc(II) cationic phthalocyanine phototoxicity, Int. J. Biochem. Cell Biol. (2013). https://doi.org/10.1016/j.biocel.2013.08.012.

[35] L.N. Milla, I.S. Cogno, M.E. Rodríguez, F. Sanz-Rodríguez, A. Zamarrón, Y. Gilaberte, E. Carrasco, V.A. Rivarola, Á. Juarranz, Isolation and characterization of squamous carcinoma cells resistant to photodynamic therapy, J. Cell. Biochem. (2011). https://doi.org/10.1002/jcb.23145.

[36] J. Friedrich, C. Seidel, R. Ebner, L.A. Kunz-Schughart, Spheroid-based drug screen: Considerations and practical approach, Nat. Protoc. (2009). https://doi.org/10.1038/nprot.2008.226.

[37] Y. Kabeya, LC3, a mammalian homologue of yeast Apg8p, is localized in autophagosome membranes after processing, EMBO J. (2000). https://doi.org/10.1093/emboj/19.21.5720.

[38] Y. Wei, S. Pattingre, S. Sinha, M. Bassik, B. Levine, JNK1-Mediated Phosphorylation of Bcl-2 Regulates Starvation-Induced Autophagy, Mol. Cell. (2008). https://doi.org/10.1016/j.molcel.2008.06.001.

[39] R. Kang, H.J. Zeh, M.T. Lotze, D. Tang, The Beclin 1 network regulates autophagy and apoptosis, Cell Death Differ. (2011). https://doi.org/10.1038/cdd.2010.191.

[40] P.J. Nadeau, S.J. Charette, J. Landry, Redox reaction at ASK1-Cys250 is essential for activation of JNK and induction of apoptosis, Mol. Biol. Cell. (2009). https://doi.org/10.1091/mbc.E09-03-0211.

[41] A. Matsuzawa, H. Ichijo, Redox control of cell fate by MAP kinase: physiological roles of ASK1-MAP kinase pathway in stress signaling, Biochim. Biophys. Acta - Gen. Subj. (2008). https://doi.org/10.1016/j.bbagen.2007.12.011.

[42] H. Kamata, S.I. Honda, S. Maeda, L. Chang, H. Hirata, M. Karin, Reactive oxygen species promote TNFα-induced death and sustained JNK activation by inhibiting MAP kinase phosphatases, Cell. (2005). https://doi.org/10.1016/j.cell.2004.12.041.

[43] L.Y. Xue, J. He, N.L. Oleinick, Promotion of photodynamic therapy-induced apoptosis by stress kinases, Cell Death Differ. (1999). https://doi.org/10.1038/sj.cdd.4400558.

[44] Y. Wang, C. Xia, Z. Lun, Y. Lv, W. Chen, T. Li, Crosstalk between p38 MAPK and caspase-9 regulates mitochondria-mediated apoptosis induced by tetra-α-(4-carboxyphenoxy) phthalocyanine zinc photodynamic therapy in LoVo cells,

Oncol. Rep. (2018). https://doi.org/10.3892/or.2017.6071.

[45] L.Y. Xue, S.M. Chiu, N.L. Oleinick, Atg7 deficiency increases resistance of MCF-7 human breast cancer cells to photodynamic therapy, Autophagy. (2010). https://doi.org/10.4161/auto.6.2.11077.

[46] M.E. Rodríguez, C. Catrinacio, A. Ropolo, V.A. Rivarola, M.I. Vaccaro, A novel HIF-1α/VMP1-autophagic pathway induces resistance to photodynamic therapy in colon cancer cells, Photochem. Photobiol. Sci. (2017). https://doi.org/10.1039/c7pp00161d.

[47] X. Duan, B. Chen, Y. Cui, L. Zhou, C. Wu, Z. Yang, Y. Wen, X. Miao, Q. Li, L. Xiong, J. He, Ready player one? Autophagy shapes resistance to photodynamic therapy in cancers, Apoptosis. (2018). https://doi.org/10.1007/s10495-018-1489-0.

[48] J.J. Reiners, P. Agostinis, K. Berg, N.L. Oleinick, D. Kessel, Assessing autophagy in the context of photodynamic therapy, Autophagy. (2010). https://doi.org/10.4161/auto.6.1.10220.

[49] E.B. Golden, I. Pellicciotta, S. Demaria, M.H. Barcellos-Hoff, S.C. Formenti, The convergence of radiation and immunogenic cell death signaling pathways, Front. Oncol. (2012). https://doi.org/10.3389/fonc.2012.00088.

[50] Y.T. Wu, H.L. Tan, G. Shui, C. Bauvy, Q. Huang, M.R. Wenk, C.N. Ong, P. Codogno, H.M. Shen, Dual role of 3-methyladenine in modulation of autophagy via different temporal patterns of inhibition on class I and III phosphoinositide 3-kinase, J. Biol. Chem. (2010). https://doi.org/10.1074/jbc.M109.080796.

[51] J. Espada, S. Galaz, F. Sanz-Rodríguez, A. Blázquez-Castro, J.C. Stockert, L. Bagazgoitia, P. Jaén, S. González, A. Cano, Á. Juarranz, Oncogenic H-Ras and PI3K signaling can inhibit e-cadherin-dependent apoptosis and promote cell

survival after photodynamic therapy in mouse keratinocytes, J. Cell. Physiol. (2009). https://doi.org/10.1002/jcp.21652.

[52] S. Martin, A.M. Dudek-Peric, A.D. Garg, H. Roose, S. Demirsoy, S. Van Eygen, F. Mertens, P. Vangheluwe, H. Vankelecom, P. Agostinis, An autophagy-driven pathway of ATP secretion supports the aggressive phenotype of BRAFV600E inhibitor-resistant metastatic melanoma cells, Autophagy. (2017). https://doi.org/10.1080/15548627.2017.1332550.

[53] F. Hirschhaeuser, H. Menne, C. Dittfeld, J. West, W. Mueller-Klieser, L.A. Kunz-Schughart, Multicellular tumor spheroids: An underestimated tool is catching up again, J. Biotechnol. (2010). https://doi.org/10.1016/j.jbiotec.2010.01.012.

[54] W. Yu, Y. Wang, J. Zhu, L. Jin, B. Liu, K. Xia, J. Wang, J. Gao, C. Liang, H. Tao, Autophagy inhibitor enhance ZnPc/BSA nanoparticle induced photodynamic therapy by suppressing PD-L1 expression in osteosarcoma immunotherapy, Biomaterials. (2019). https://doi.org/10.1016/j.biomaterials.2018.11.019.

[55] M.C. Maiuri, G. Le Toumelin, A. Criollo, J.C. Rain, F. Gautier, P. Juin, E. Tasdemir, G. Pierron, K. Troulinaki, N. Tavernarakis, J.A. Hickman, O. Geneste, G. Kroemer, Functional and physical interaction between Bcl-XL and a BH3-like domain in Beclin-1, EMBO J. (2007). https://doi.org/10.1038/sj.emboj.7601689.

[56] S. Pattingre, A. Tassa, X. Qu, R. Garuti, H.L. Xiao, N. Mizushima, M. Packer, M.D. Schneider, B. Levine, Bcl-2 antiapoptotic proteins inhibit Beclin 1-dependent autophagy, Cell. (2005). https://doi.org/10.1016/j.cell.2005.07.002.

[57] M. Djavaheri-Mergny, M.C. Maiuri, G. Kroemer, Cross talk between apoptosis and autophagy by caspase-mediated cleavage of Beclin 1, Oncogene. (2010).

https://doi.org/10.1038/onc.2009.519.

[58] S. Luo, D.C. Rubinsztein, Apoptosis blocks Beclin 1-dependent autophagosome synthesis: An effect rescued by Bcl-xL, Cell Death Differ. (2010). https://doi.org/10.1038/cdd.2009.121.

A

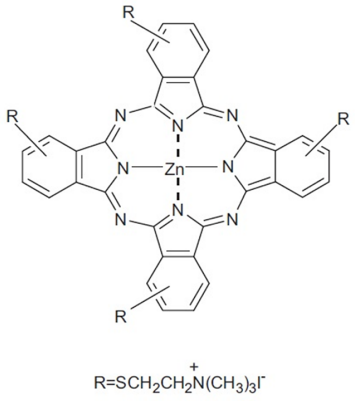

B

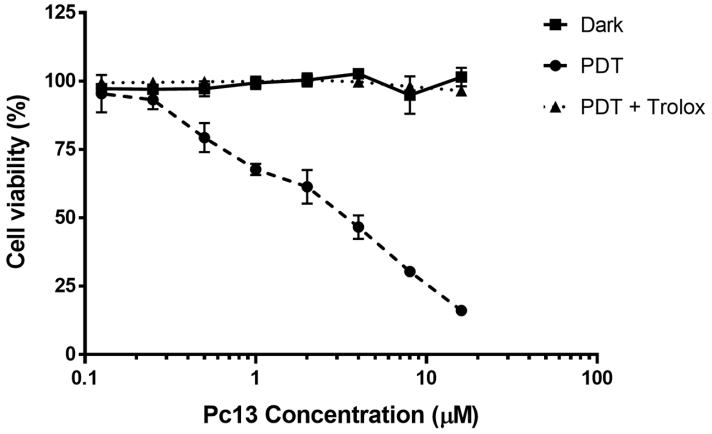

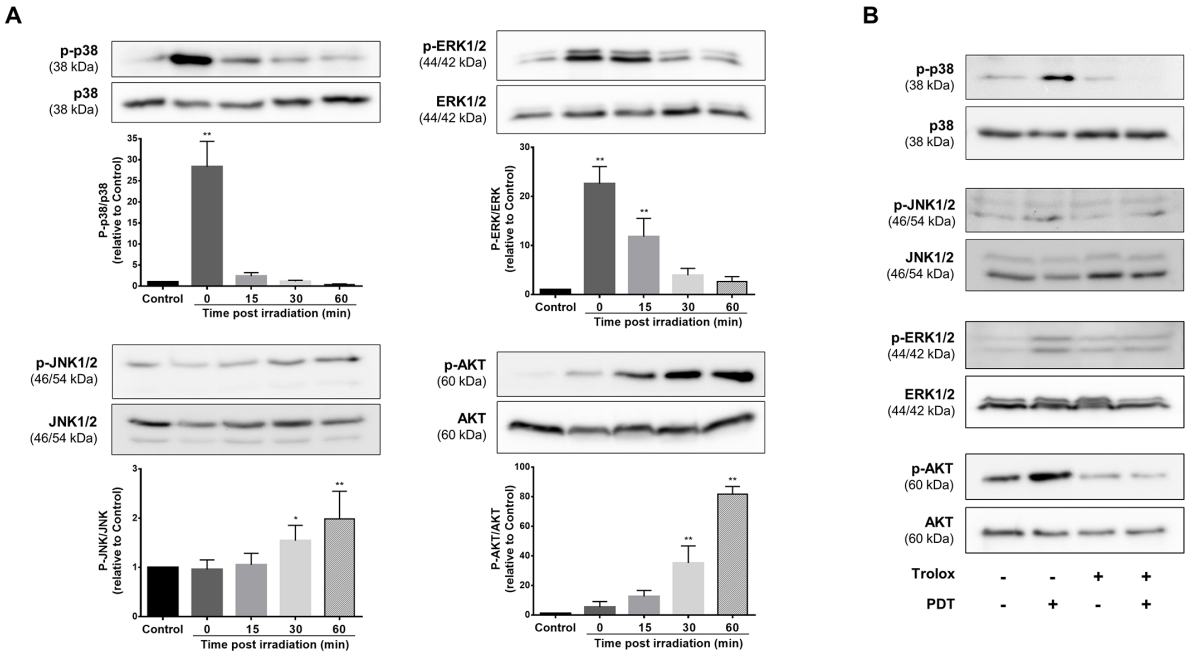
A
p-p38
(38 kDa)
p38
(38 kDa)
P-p38/p38
(relative to Control)
Control
0
15
30
60
Time post irradiation (min)
p-ERK1/2
(44/42 kDa)
ERK1/2
(44/42 kDa)
P-ERK/ERK
(relative to Control)
p-JNK1/2
(46/54 kDa)
JNK1/2
(46/54 kDa)
P-JNK/JNK
(relative to Control)
p-AKT
(60 kDa)
AKT
(60 kDa)
P-AKT/AKT
(relative to Control)
B
p-p38
(38 kDa)
p38
(38 kDa)
p-JNK1/2
(46/54 kDa)
JNK1/2
(46/54 kDa)
p-ERK1/2
(44/42 kDa)
ERK1/2
(44/42 kDa)
p-AKT
(60 kDa)
AKT
(60 kDa)
Trolox
PDT

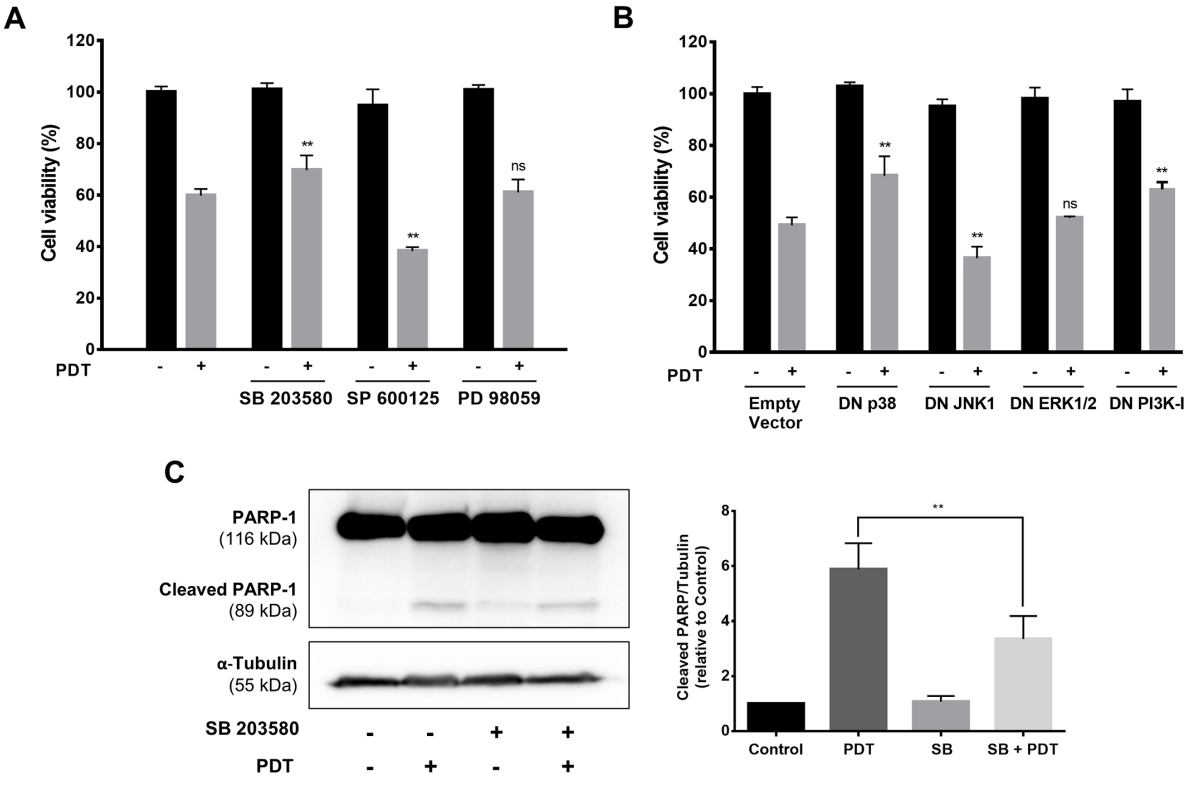

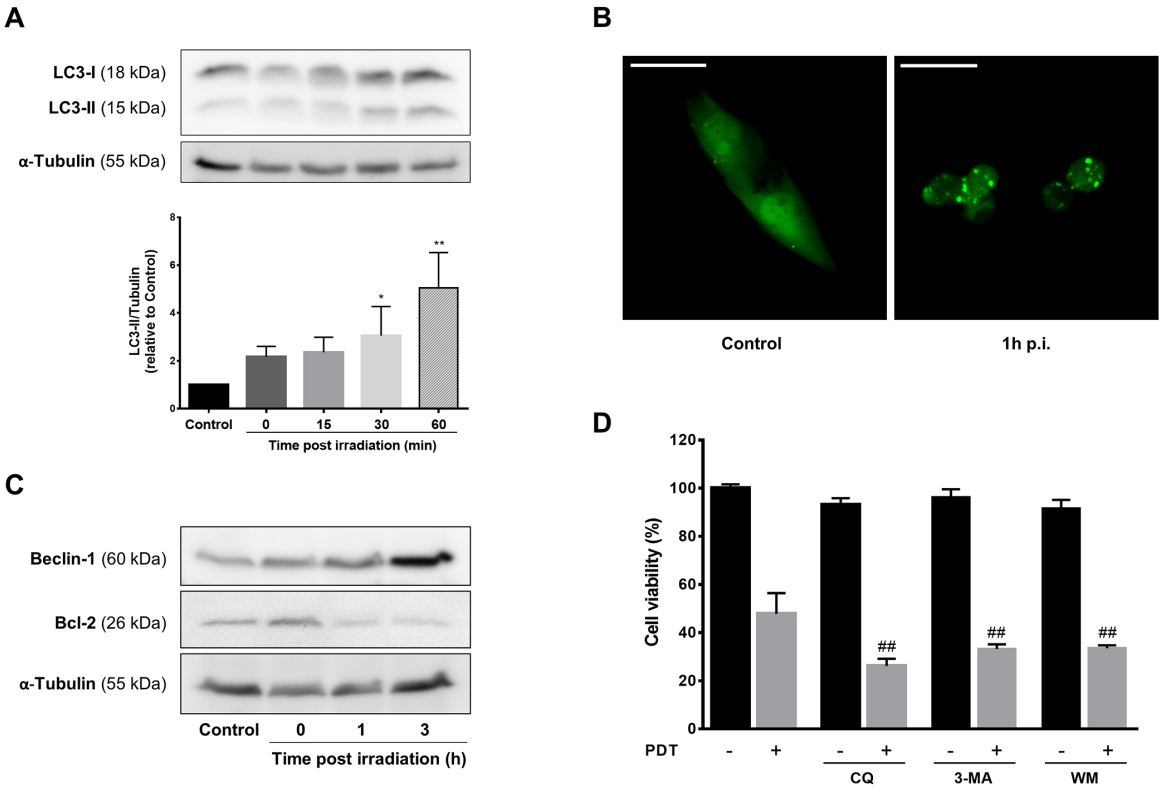

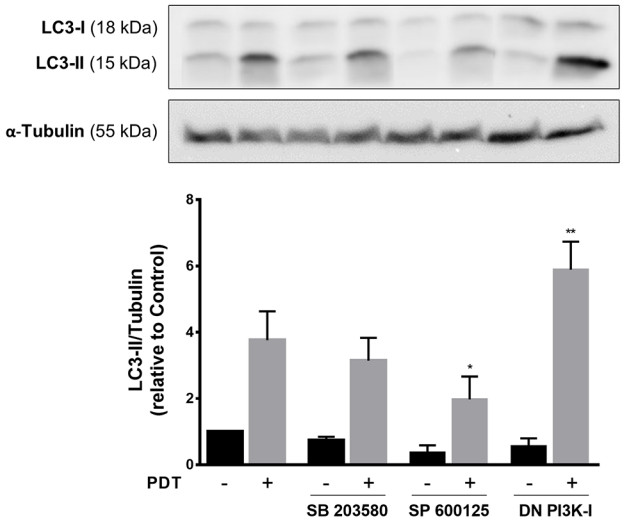

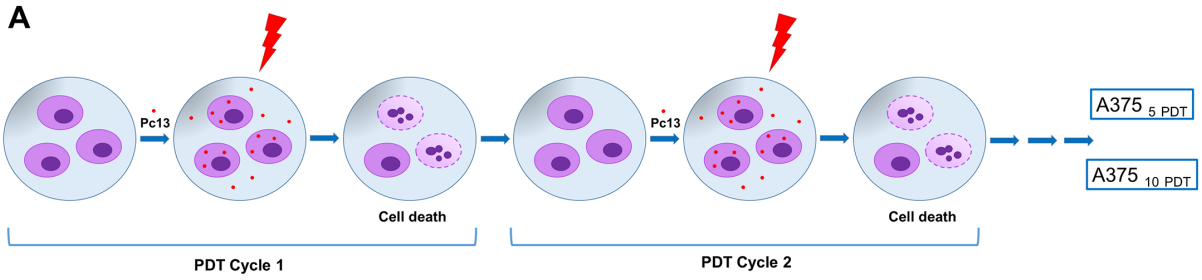

B

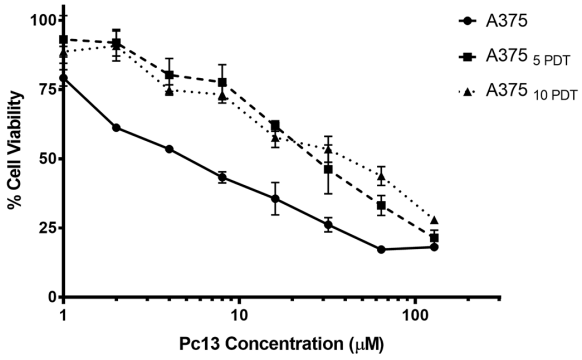

Cell line	IC_{50} (μM)
A375	3.6 ± 0.2
A375 $_{5\ PDT}$	21.5 ± 5.0*
A375 $_{10\ PDT}$	26.5 ± 5.7**

C

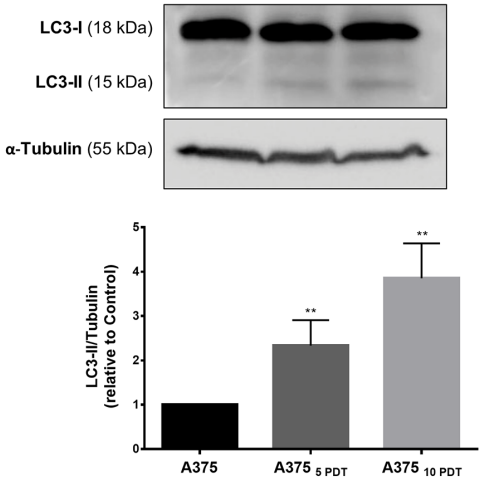

D

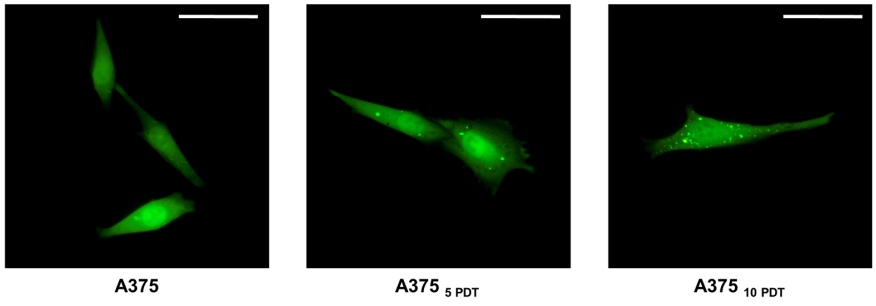

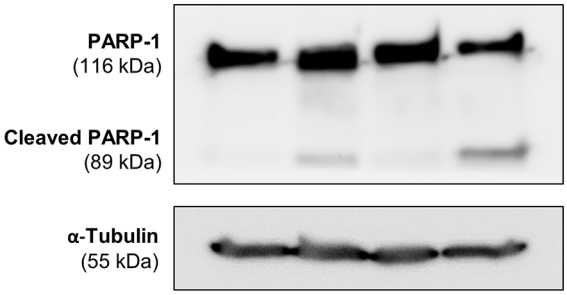

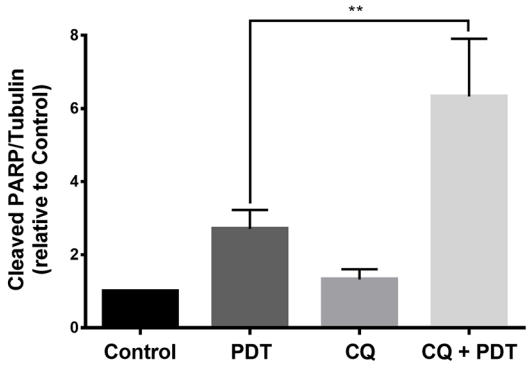

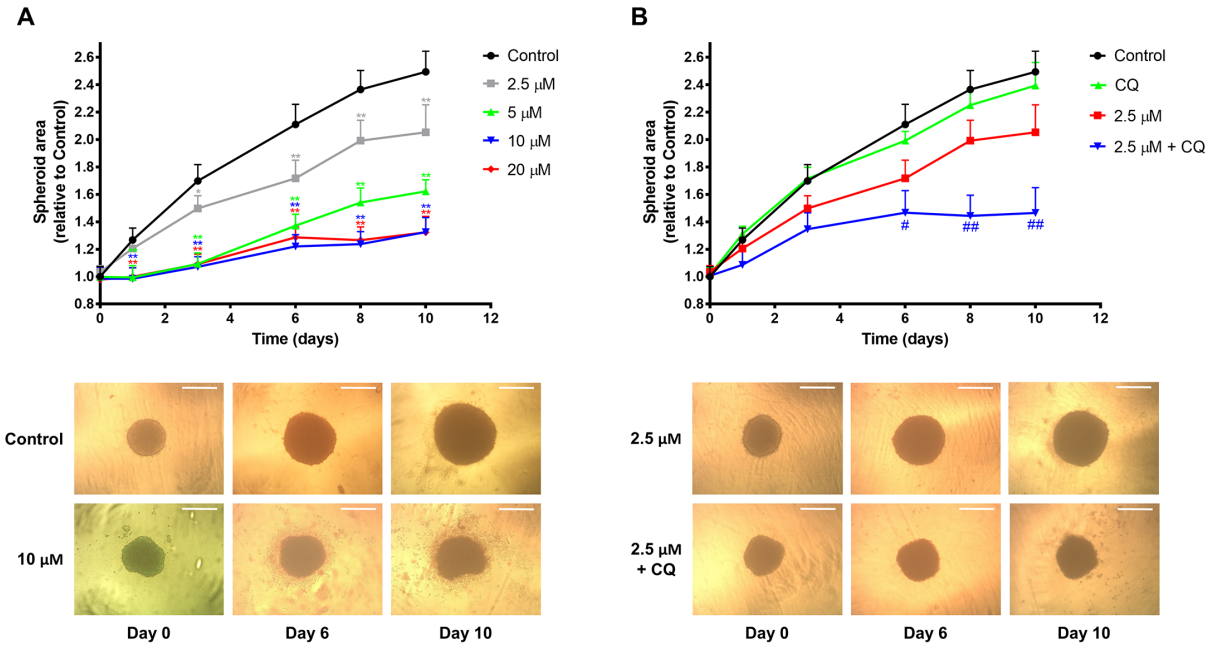
A
Spheroid area (relative to Control)
Time (days)
Control
2.5 μM
5 μM
10 μM
20 μM
B
Spheroid area (relative to Control)
Time (days)
Control
CQ
2.5 μM
2.5 μM + CQ
Control
10 μM
2.5 μM
2.5 μM + CQ
Day 0
Day 6
Day 10

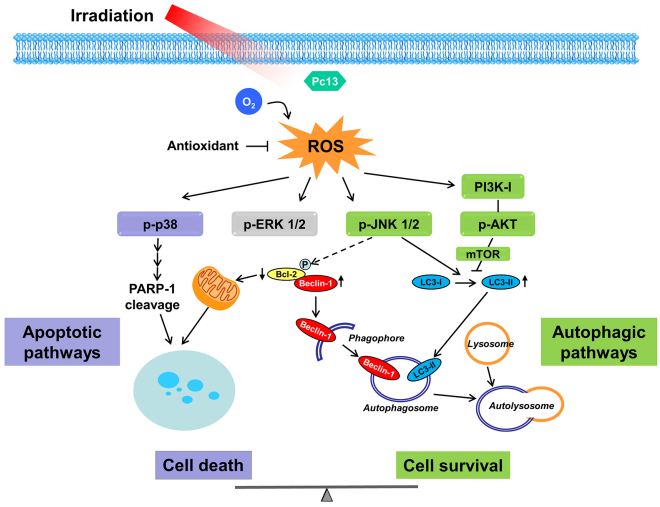

Highlights

- Pc13 is a potent photosensitizer in 2D and 3D melanoma cultures

- Oxidative stress induced by Pc13 PDT activates p38, JNK, ERK and PI3K-I/AKT pathways

- Pc13 PDT triggers apoptosis through p38 pathway

- JNK and PI3K-I/AKT pathways regulate Pc13 PDT-induced autophagy

- Inhibition of autophagy potentiates the Pc13 apoptotic response